

Thermodynamic entropy production fluctuation in a two dimensional shear flow model

F. Bonetto[†], J.L. Lebowitz[‡]

Abstract: We investigate fluctuations in the momentum flux across a surface perpendicular to the velocity gradient in a stationary shear flow maintained by either thermostated deterministic or by stochastic boundary conditions. In the deterministic system the Gallavotti-Cohen (GC) relation for the probability of large deviations, which holds for the phase space volume contraction giving the Gibbs ensemble entropy production, never seems to hold for the flux which gives the hydrodynamic entropy production. In the stochastic case the GC relation is found to hold for the total flux, as predicted by extensions of the GC theorem but not for the flux across part of the surface. The latter appear to satisfy a modified GC relation. Similar results are obtained for the heat flux in a steady state produced by stochastic boundaries at different temperatures.

1. Introduction

There has been much effort during the past decade to connect statistical mechanics of stationary nonequilibrium states (SNS) with the theory of dissipative dynamical systems [1]. While most results obtained so far via this approach are more of a mathematical than physical interest there is one potential exception: the Gallavotti-Cohen theorem [2] and its generalizations [3][4][5]. The original GC theorem was motivated by the numerical results of [6] on a “thermostated” dynamical system. The phase-space time evolution of such a system is given by an equation of the form

$$\dot{X} = \mathcal{F}(X) \tag{1.1}$$

with \mathcal{F} chosen to keep $X(t)$ confined to a compact surface Σ in the phase-space while forcing the system into a nonequilibrium state. The latter requires that \mathcal{F} be non-hamiltonian with $\text{div}\mathcal{F}(X) = \sigma(X) \neq 0$.

Using some very strong assumptions on the dynamical system (1.1), GC proved that in the SRB measure [7] describing the SNS of this system the probability distribution $P_\tau(p) = \langle \delta(p - \pi_\tau(X)) \rangle$ of

$$\sigma_\tau(X) = \frac{1}{\tau \langle \sigma \rangle} \int_{-\tau/2}^{\tau/2} \sigma(X(t)) dt \tag{1.2}$$

satisfies the equality

$$\lim_{\tau \rightarrow \infty} \frac{1}{\tau \langle \sigma \rangle} \ln \frac{P_\tau(p)}{P_\tau(-p)} = p. \tag{1.3}$$

Here $\langle \cdot \rangle$ represents the average in the SNS.

The quantity $\langle \sigma \rangle$ is formally equal to the “rate of change” of the Gibbs entropy in the SNS. More precisely, if we start the system with a measure $\mu_0(dX) = \rho_0(X)dX$ where dX is the Liouville measure restricted to the surface Σ then, using the evolution (1.1),

$$\dot{S}_G(t) = -\frac{d}{dt} \int \rho_t \log \rho_t dX = \mu_t(\sigma) \xrightarrow{t \rightarrow \infty} \langle \sigma \rangle \tag{1.4}$$

where the existence of the limit will hold under the assumptions of the GC theorem. Furthermore we will have $\langle \sigma \rangle < 0$ implying that $S_G(t) \rightarrow -\infty$ whenever the limiting state is not an equilibrium one with zero currents [8],[9].

[†]Mathematics Department, Rutgers University, New Brunswick, NJ 08903, email: bonetto@math.rutgers.edu.

[‡]Mathematics and Physics Department, Rutgers University, New Brunswick, NJ 08903, email: lebowitz@math.rutgers.edu.

Based on the relation (1.4) $\sigma_\tau(X)$ is often called the (normalized) “average entropy production during a time interval τ ” in the SNS. The identification of σ_∞ , the object of the GC theorem, with entropy production was further strengthened by the form of $\sigma(X)$ in many examples of bulk thermostated systems, e.g. those considered by Moran and Hoover [10] for electrical conduction and by [11] for shear flow. In those systems $\sigma(X)$ is given by an expression related to the hydrodynamic entropy production and the validity of the GC relation, eq.(1.3), was confirmed by numerical simulations, despite the fact that the conditions of the GC theorem are not satisfied there.

Such bulk thermostated systems are however very different from realistic systems which are typically driven to SNS by inputs at their boundaries: the motion in their interiors being governed by Hamiltonian dynamics which do not produce any phase space volume contraction. It is therefore important, for comparison with real systems, to consider models of dynamical systems in which the thermostats forcing the system into SNS operate only near the boundaries. Such deterministic models were introduced by Chernov and Lebowitz [12] for shear flow and by Gallavotti [1], and van Beijeren [13] for heat flux. In this paper we investigate the validity and possible generalizations of the GC relation for such boundary driven systems. Before doing that we note that the GC theorem has been extended to open systems in contact with infinite thermal reservoirs which act on the system but are not changed by it. The simplest modeling of such a situation is via stochastic transitions, induced by the reservoirs, between different microstates of the system induced by the reservoirs [4]. Thus, to model a system carrying a heat current and/or a momentum flux, one may use Maxwellian boundary conditions. This means that a particle hitting the left (right) wall will be reflected with a Maxwellian distribution of velocities corresponding to temperatures T_L (T_R) and mean velocities u_L (u_R) parallel to these walls. For $T_L \neq T_R$ this will induce a SNS with a heat flux while $u_L \neq u_R$ will (using periodic boundary conditions in the flow directions) induce a SNS with a shear flow, see [14][15]. It is expected (hoped) that the deterministic (thermostated) and stochastic kinds of boundary modeling will yield similar SNS of a macroscopic system away from the boundaries. This is what happens in equilibrium systems, at least when not in a phase transition region.

Such an “equivalence of ensembles” is far from established for SNS. In fact there is, at some level, a profound difference between thermostated and stochastically modeled SNS as far as S_G is concerned. As readily noted the former have $S_G(t) \rightarrow -\infty$, and $\dot{S}_G(t) \rightarrow \langle \sigma \rangle < 0$, while the latter have $S_G(t) \rightarrow \bar{S}_G$, $\dot{S}_G(t) \rightarrow 0$. The origin of the difference lies in the differences in the measures describing these SNS. Thermostated SNS are described by an SRB measure which is singular with respect to the induced Lebesgue measure dX , while the SNS of stochastically driven systems are (this can be proven in some case and expected in general) described by measures that are absolutely continuous with respect to dX [16][17]. This difference need not however mean much for a macroscopic system, since quantities of physical interest are sums of functions which depend only on a few variables. Their properties are therefore determined by the reduced distribution functions which can be expected to be absolutely continuous with respect to the local Lebesgue measure, i.e. expressible as densities, even when the full measure is singular and fractal [18].

Interestingly enough, it is possible for the boundary driven pure heat flow case to model the thermostat in such a way that the expression for $\sigma(X)$ appearing in the GC relation is the same, up to terms whose average vanishes, for both the deterministic and stochastic case, see [1]. It can be written as

$$\sigma = \left(\frac{1}{T_L} - \frac{1}{T_R} \right) J_Q + \frac{dF(X)}{dt} \quad (1.5)$$

so that

$$\langle \sigma \rangle = \left(\frac{1}{T_L} - \frac{1}{T_R} \right) \langle J_Q \rangle \quad (1.6)$$

where $J_Q(X)$ is the heat flux through some surface in the middle of the system and the average of the time derivative dF/dt vanishes in the SNS. $\langle \sigma \rangle$ has the form of entropy production in the left and right heat “reservoirs” which is also equal to the hydrodynamic entropy production in the SNS [15].

The situation is different for the thermostated boundary driven shear flow case considered by [12]. The $\sigma(X)$ in (1.2), entering the GC theorem for that model is not clearly related to the hydrodynamic entropy production. The latter corresponds now to a momentum flux through the system, $J_M(X)$, for which a GC relation holds for the stochastically driven system. The question is then whether there is still enough equivalence between systems driven deterministically and stochastically so that the GC relation for $J_M(X)$, derived for the latter, also holds in the former.

Another question which concerns both the heat conduction and the shear case is whether the GC relation can be observed in real macroscopic physical systems. More precisely, we know that in the linear regime the GC

relations imply an Onsager type reciprocity relations for the transport coefficients [19], [4] which hold not only globally but also locally. Our question is therefore the following: assuming that the GC relation holds for some flux crossing a surface S does it also hold (in some form) for the flux through part of S . The reason this is important for the applicability of the GC relation to real system is that for values of p for which $P_\tau(p)$ is of order unity, $P_\tau(-p)$, in eq. (1.3), which corresponds to the flux J going in the opposite direction from its usual one, e.g. the heat flowing from the cold to the hot reservoir, is so small in a macroscopic system that the possibility of observing it is effectively zero. A local flux reversal on the other hand may be quite observable: an attempt in this direction was indeed made by Ciliberto and Laroche [20].

Here we describe numerical investigations of these questions for a deterministic and stochastically driven shear flow SNS and for a stochastic heat flow model.

2. Description of the shear flow model

Deterministic: The system consists of N unit mass particles contained in a $L \times M$ box with periodic boundary conditions in the x -direction and reflecting boundaries on the walls perpendicular to the y -direction. The dynamics in the bulk of the system is Hamiltonian with hard core interactions (the particles have a radius r). When a particle collides with the reflecting walls its outgoing speed is the same as the incoming one while the direction of the velocity is chosen in a way which simulates a moving boundary and creates a shear flow. The boundary transformation we consider is the same as in [12][21]. Let ϕ and ψ be the angle that the incoming (outgoing) velocity forms with the positive x -direction if the particle collides with the upper wall or with the negative x -direction if the particle collides with the lower wall. In the thermostated system the outgoing angle ψ is given by a function of the incoming angle ϕ : $\psi = f(\phi)$. The function f we choose is $f(\phi) = (\pi + b) - \sqrt{(\pi + b)^2 - \phi(\phi - 2b)}$. This is time-reversible, i.e. $\pi - f(\pi - f(\phi)) = \phi$ see Fig. 1.

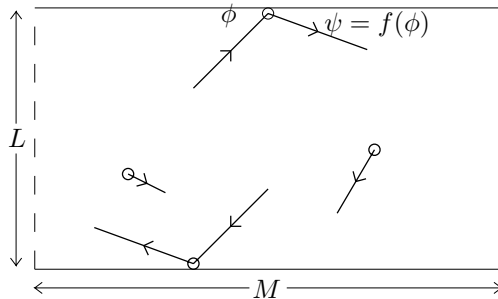


Fig. 1: Schematic representation of the dynamics of the system.

Stochastic: The dynamics in the interior of the system is the same as before while the outgoing velocity at the upper (lower) wall is now chosen as if the particle was coming from a Maxwellian bath at temperature β^{-1} moving at velocity $v_0(-v_0)$. More precisely we assume that after a collision with the boundary the particle emerges with a velocity that is randomly chosen from a distribution:

$$\mathcal{P}(v) = \frac{1}{Z} v_y \exp\left(\frac{\beta}{2} \left((v_x - \epsilon_y v_0)^2 + v_y^2\right)\right) \quad (2.1)$$

where Z is a normalization constant, v_0 is the mean x -momentum of the particle after a collision and ϵ_y is 1 if the collision is with the upper wall and -1 if it is with lower wall.

In [21] we checked the validity of the GC relation for the phase space contraction generated during the collisions of particles with the deterministic thermostated boundary. We divided the phase space contraction into a contribution due to the lower boundary and one due to the upper one. We found that the GC relation was well verified for the total phase space contraction $\sigma(X)$ but not for the partial ones¹.

¹ We observe that based on the proof of GC we have no reason to expect that such a relation should hold for the partial phase space contraction. We tested it anyway since, as already noted, the GC relation appears to hold in more general situations than those covered by the GC theorem, e.g. for the total σ here.

As already noted there is no apparent connection between the phase space contraction and the hydrodynamic entropy production which is proportional to the flux of the x -component of the momentum across the system. In [12] equality between average phase space contraction rate and average hydrodynamical entropy production rate was shown to hold to first order in the shear in the limit in which the system becomes large (at constant density), *i.e.* macroscopic, but the shear rate goes to zero in such a way as to maintain a constant total momentum transfer. This was done under the assumption that before a collision with either wall the particle velocities are distributed according to a Maxwellian. The equality between these averages was supported by numerical evidence.

In the present paper we further investigate the possible equivalence between phase space contraction and entropy production. The momentum flux is equal to the momenta carried by particles crossing a line through the middle of the system plus the exchange of momentum between two colliding particles when their center are on opposite side of the line, see fig.2.

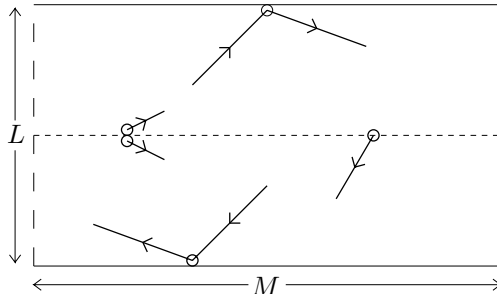


Fig. 2: Events producing momentum flux.

To be more precise we first introduce a discrete time for the system (in a slightly different way from what we did in [21]). Let $X = (q_i, v_i)$ a phase space point, $\Phi_t(X)$ be the time evolution induced by the dynamics and let $\tau(X)$ be the first time at which a particle crosses the middle line or two particles on different sides of this line collide starting from the phase point X (we call such a situation a *timing event*) and let $S(X) = \Phi_{\tau(X)}(X)$. Finally let $\pi(X)$ be the exchange of x -momentum at the phase point X .

We now specify the quantity whose fluctuations we will check. Given an integer τ let

$$\pi_\tau(X) = \sum_{i=-\tau/2}^{\tau/2} \pi(S^i(X)) \quad (2.2)$$

and

$$p_\tau(X) = \frac{\pi_\tau(X)}{\langle \pi_\tau(X) \rangle} \quad (2.3)$$

where the mean $\langle \cdot \rangle$ is taken with respect to the stationary measure of the system. Let now $\Pi_\tau(p)$ be the distribution function of $p_\tau(X)$ and

$$\xi_\tau(p) = \frac{1}{\langle \pi_\tau(X) \rangle} \ln \left(\frac{\Pi_\tau(p)}{\Pi_\tau(-p)} \right).$$

We can formulate our “GC fluctuation relation for the entropy production” as follows:

$$\lim_{\tau \rightarrow \infty} \xi_\tau(p) = Cp \quad (2.4)$$

Here C is the conversion constant between momentum flow and entropy production that, from hydrodynamics [21], is $C = 2u_b/T_b$ where u_b is the velocity of the particle near the upper boundary and T_b is the temperature near the boundary. Observe that this as well as the following definitions, make sense also in the stochastic case when the phase space contraction rate is not defined.

In this setting we define a local entropy production by looking at all events like the ones described in figure 2 that happen in a specified part of the middle line of size lL . More precisely let

$$\pi^l(X) = \pi(X)\chi_{[0, lL]}(X) \quad (2.5)$$

where $\chi_A(X) = 1$ if the location of the momentum transfer event is at a point in A and 0 otherwise. We now define in a way analogous to eqs.(2.2) and (2.3) the quantities $\pi_\tau^l(X)$, $p_\tau^l(X)$, $\Pi_\tau^l(p)$ and $\xi_\tau^l(p)$ and state our “local GC relation” for the entropy production as,

$$\lim_{\tau \rightarrow \infty} \xi_\tau^l(p) = Cp \quad (2.6).$$

More generally we check if a relation of the form:

$$\lim_{\tau \rightarrow \infty} \xi_\tau^l(p) = C_l p \quad (2.7)$$

holds.

The stochastic model permits us to discuss also different kind of transport phenomena. In fact we can set the reciprocal temperature β of the upper and lower walls to different value β^+ and β^- . In this case we will have also transport of heat through the middle of the system. We ran simulation also for this case, setting $v_0 = 0$ for simplicity, and report the results in section 4. Clearly now the correct quantity to compute is the energy transferred across the middle line when a particle crosses or a collision happens.

3. Numerical experiments for the shear flow

We simulated systems with $N = 20, 40$ and 60 particles and L, M such that the number density $\delta = N/LM = 0.034$ was fixed. We chose two different ways to set L and M . In one case we fix $L = M$ *i.e.* a square domain. In the second case we keep M fixed at the value it had for $N = 20$ and increase L proportionally as N is increased. In the deterministic case we fixed the energy per particle $\frac{1}{2N} \sum_i v_i^2 = 1$ while in the stochastic case we fixed the values of v_0 and β to reproduce the mean velocity u_b and temperature $T_b = \langle (v - u)^2 \rangle$ observed in the $N = 60$ simulation for the deterministic system. More precisely we fixed $v_0 = 0.2$ and $\beta^{-1} = 0.48$. Finally the radius r was fixed to 1. For each value of N and L we followed a single trajectory of the system for $5 \cdot 10^8$ timing events and used it to compute the distributions $\Pi_\tau^l(p)$. As in [21] (differently than in [22]) we did not discard any events between two consecutive segments of length τ .

3.1. Stochastic case

As discussed in the introduction (see also section 5.1 for further discussion) we expect the fluctuation relation to hold for the total momentum flux corresponding to the hydrodynamic entropy production. This can indeed be seen in figure 3 in which $\xi_\tau(p)$ is plotted for $\tau = 300$ and $N = 60$ for the rectangular geometry. The dashed line represent the theoretical prediction $\xi_\infty(p) = 0.769p$. Similar results hold for $N = 20$ and $N = 40$.

The relation in the strong form given by eq.(2.6) appears not to hold for $l < 1$ but eq.(2.7) seems to hold as one observes a linear behavior of $\xi_\tau^l(p)$ always in Fig. 3.

The results for ξ_τ^l can be used to obtain the behavior of the slope C_l as a function of l . We report the result in Fig. 4 for the three value of N and the two different geometries we have used. We observe that in the case in which we keep the box square C_l decrease with N and seems to reach a limit different from 1 when N grows. If we just increase the horizontal side of the box keeping its height constant C_l increases with N and it is not clear from the data what, if any, limit is reached when $N \rightarrow \infty$.

Instead of fixing l we also tried fixing the length $l * L$ but found nothing interesting.

3.2. Deterministic case

The situation looks very different in the deterministic case. No fluctuation relation seems to hold even when we consider the full momentum transfer. The result are shown in Fig. 5 where $\xi_\tau(p)$ is plotted for $\tau = 100, 200$ and 300 . The dashed line represents the value predicted by eq. (2.4). Although we still observe a linear behavior, the slope appears to be increasing with τ so that no limit seems to be reached. We will attempt an explanation of this phenomenon in the last section.

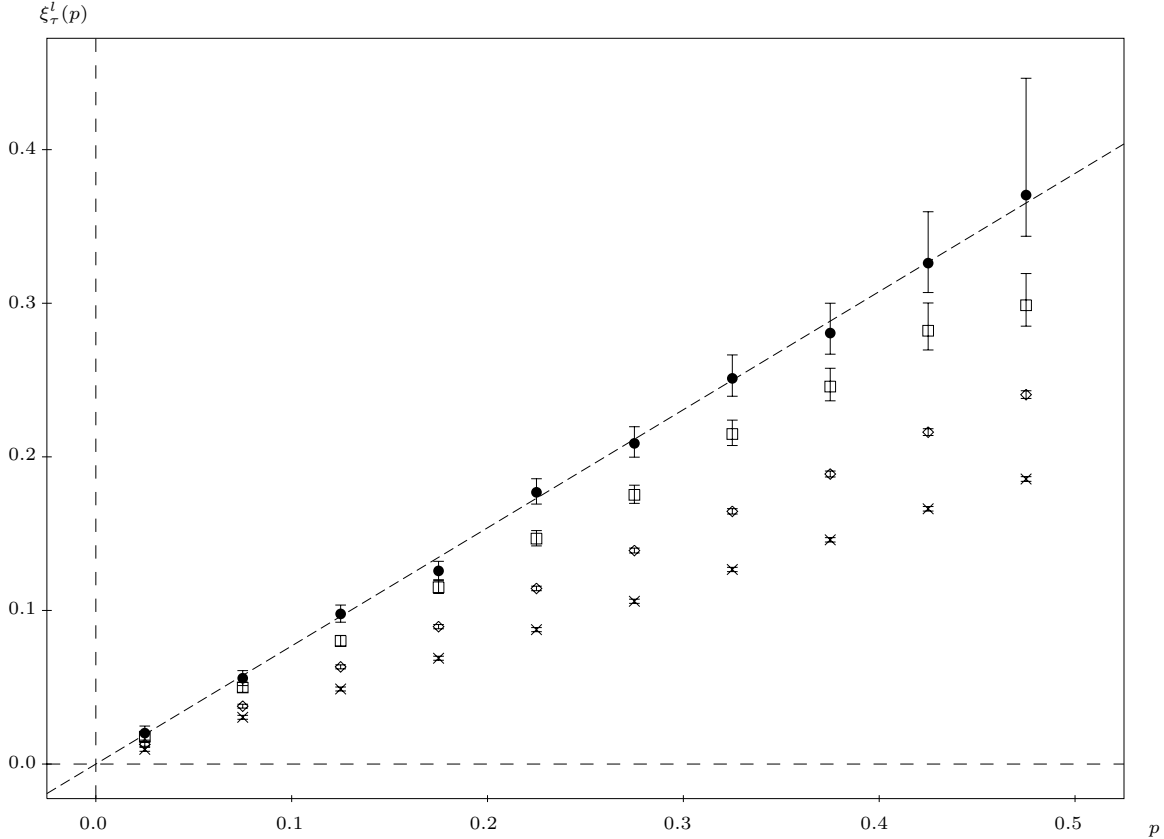


Fig. 3: Fluctuation relation for the momentum flux in the stochastic shear flow with rectangular geometry. The filled circles (\bullet) represent the experimental value for the total momentum flux, with error bars, for $\tau = 400$ and $N = 60$ while the dashed line is the theoretical prediction. The other data represent the partial fluctuation relation for $l = 0.9$ (\square), $l = 0.6$ (\diamond) and $l = 0.3$ (\times). In all three cases $\tau = 400$.

We observe that a relation like eq. (2.7) seems to hold if we look at the partial momentum flux. This is clearly shown in Fig. 6 where the behavior of $\xi_\tau^l(p)$ for $l = 0.6$ and several values of τ is plotted for $N = 60$ in the rectangular geometry. As in the stochastic case we can look at the behavior of C_l as a function of l for both geometries. The results are plotted in Fig. 7. As can be seen the slope depends only very weakly on the size of the system, at least for the square geometry. The only value for which C_l seems to depend on the size is for $l = 0.9$.

It is interesting to observe that if the fluctuation relation was true we would expect to observe a slope $C_l = 2u_b/T_b$ as discussed for the stochastic system. In this situation, and mainly for the square geometry, the value of u_b varies significantly from $N = 20$ to $N = 60$ while C_l remain almost constant. This and the result for the total momentum transfer suggests that the fluctuation of the phase space contraction rate and those of the momentum flux behave differently.

4. Heat flow

The stochastic boundary condition permits us to study the case in which the two walls are kept at different temperatures T_+ and T_- . In this case the hydrodynamics entropy production is proportional to the heat current or energy flux from the upper wall of the system to the lower one. The events contributing to an exchange of energy are the same as those considered in Fig. 2 but now we consider the kinetic energy of a particle passing through the middle line or the exchange of energy in a collision between two particle that are on different side of the middle line.

Analogously to what we did in section 2 we define $\varepsilon(X)$ as the energy exchange for a point X that is on the

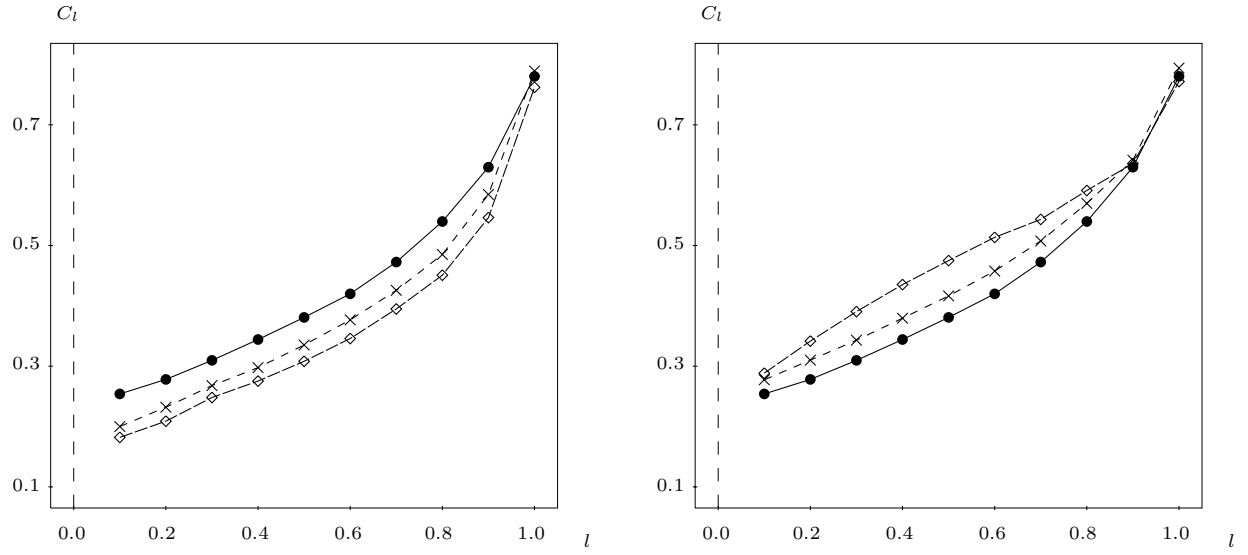


Fig. 4: Slope C_l as a function of l in the stochastic shear flow for $N = 20$ (\bullet), $N = 40$ (\times) and $N = 60$ (\diamond). The left figure is for the square geometry while the right one is for the rectangular geometry.

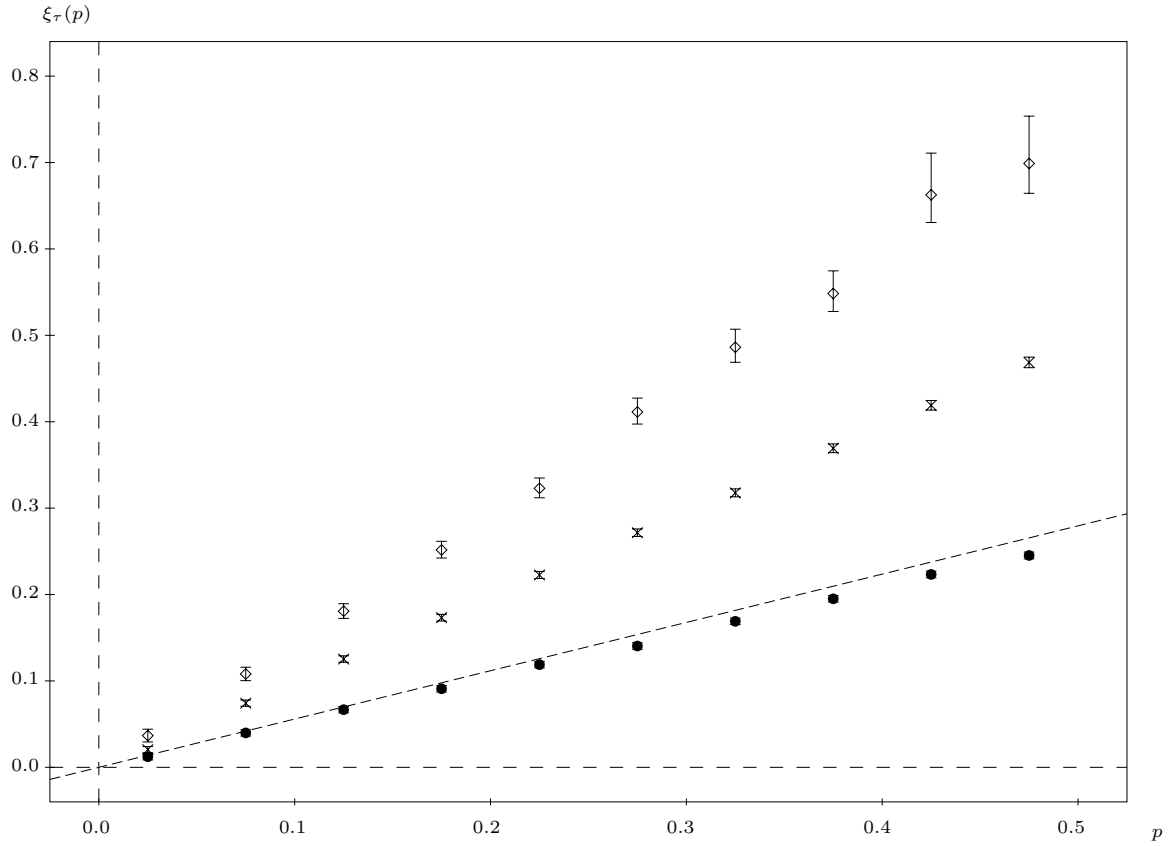


Fig. 5: Fluctuation relation in the deterministic shear flow in the rectangular geometry for the total momentum flux with $\tau = 100$ (\bullet), $\tau = 200$ (\times) and $\tau = 300$ (\diamond).

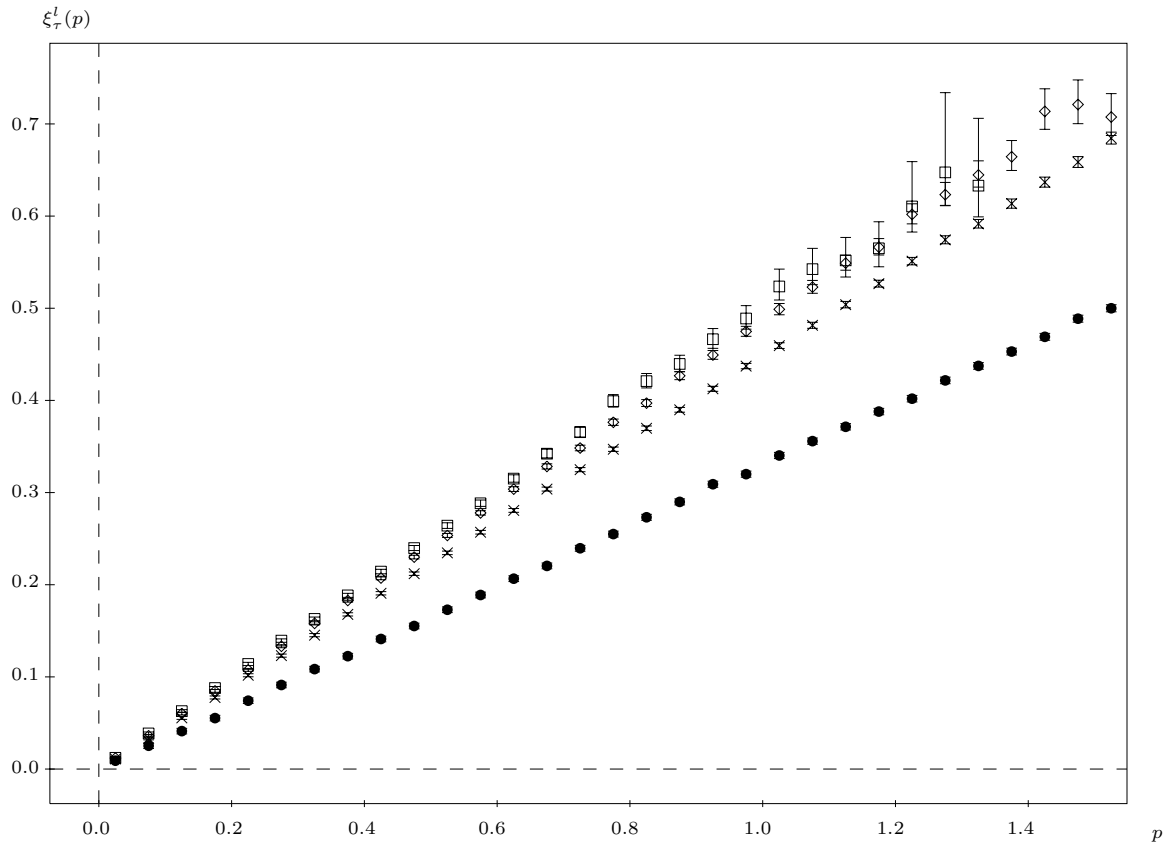


Fig. 6: Approach to a limit of the right hand side of eq.(2.7) for the deterministic case. In this case $l = 0.6$ while $\tau = 100$ (\bullet), 300 (\times), 500 (\diamond) and 700 (\square).

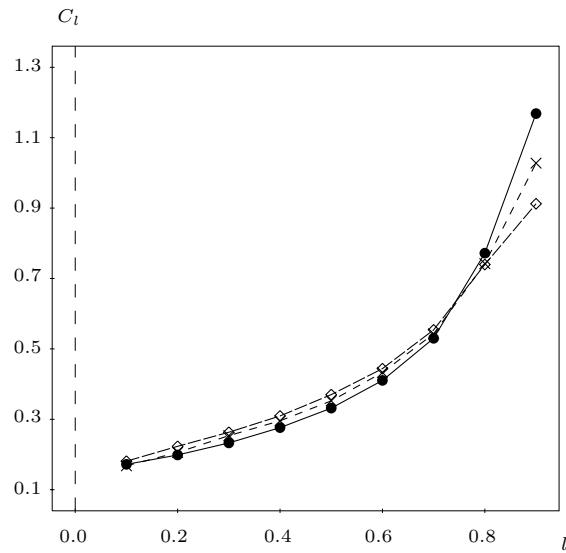


Fig. 7: Slope C_l as a function of l in the deterministic shear flow for $N = 20$ (\bullet), $N = 40$ (\times) and $N = 60$ (\diamond) in the rectangular geometry. The graph of the square geometry is analogous.

Poincaré section with

$$\varepsilon_\tau(X) = \sum_{i=-\tau/2}^{\tau/2} \varepsilon(S^i(X)) \quad (4.1)$$

and

$$e_\tau(X) = \frac{\varepsilon_\tau(X)}{\langle \varepsilon_\tau(X) \rangle} \quad (4.2)$$

Let now $E_\tau(e)$ be the distribution function of $e_\tau(X)$ and

$$\xi_\tau(e) = \frac{1}{\langle \varepsilon_\tau(X) \rangle} \ln \left(\frac{E_\tau(e)}{E_\tau(-e)} \right)$$

As before we expect that

$$\lim_{\tau \rightarrow \infty} \xi_\tau(e) = Ce \quad (4.3)$$

where C is the proper conversion constant between heat flow and entropy production:

$$C = \frac{1}{T_+} - \frac{1}{T_-}$$

Similarly we define $\varepsilon_l(X)$, $e_l(X)$, $E_\tau^l(e)$ and $\xi_\tau^l(e)$ and check whether

$$\lim_{\tau \rightarrow \infty} \xi_\tau^l(e) = C_l e \quad (4.4)$$

The numerical experiments are very similar to the ones described in section 3 but we considered only stochastic boundary conditions with rectangular geometry. Finally we fixed $T_+ = 0.7$, $T_- = 0.4$ and all the other parameters as in the shear flow case. The global fluctuation relation is shown in figure 8. There it can be observed that the fluctuations are smaller than the shear flow case. In fact for $\tau = 300$, when in the shear flow case the limiting behavior was reached, we have just 2 points for the fluctuation. We interpret the results as showing an approach to the expected limit. Similar result are obtained for $N = 40, 60$. The plots for the $\xi_\tau^l(e)$, again, appear very linear, and their slopes C_l are shown in figure 9.

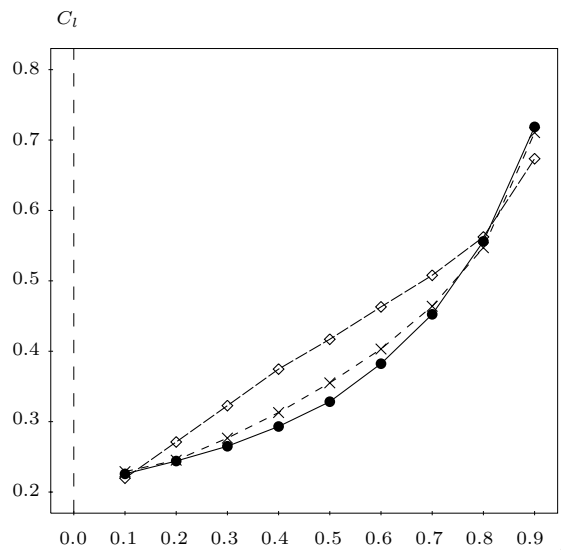


Fig. 9: Slope C_l as a function of l in the heat flow model for $N = 20$ (\bullet), $N = 40$ (\times) and $N = 60$ (\diamond).

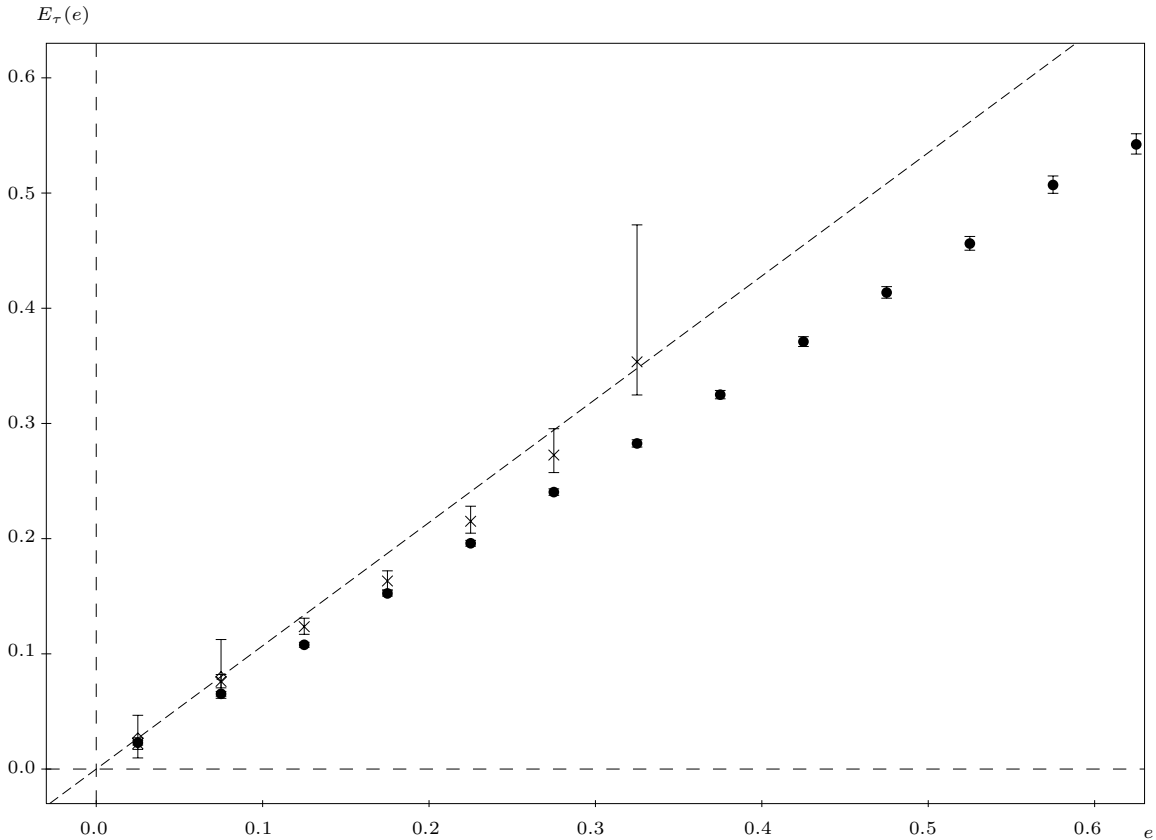


Fig. 8: Fluctuation relation for the total energy flux in the heat flow model. The experimental value are plotted with error bar for $\tau = 100$ (\bullet), $\tau = 200$ (\times) and $\tau = 300$ (\diamond) and $N = 20$. The dashed line is the theoretical prediction.

Similar comments as the one for the rectangular geometry shear flow hold here.

5. Conclusions

We now try to summarize the results of our numerical experiments.

5.1. Global fluctuation

In the case of the stochastic boundary conditions the GC relation appears to be satisfied for both shear flow and heat conduction. This is not surprising. As in [4], [5], [15] we consider the stationary probability $P_\tau(X(t))$ on the space of the trajectories of the system from time $-\tau$ to time τ . (This can be assumed to be unique, see for example [16], [23].) Define then the time reversal operation $I((q_i, v_i)) = (q_i, -v_i)$ then if $X(t)$ is a possible trajectory so is $I(X(t))$ and we can consider the measure $\bar{P} = I^*P$. Then as in [4], [5] one finds

$$\frac{dP}{d\bar{P}}(X) = \exp \left\{ R(X(\tau)) - R(X(-\tau)) + \int_{-\tau}^{\tau} \sigma(X(t)) dt \right\} \quad (5.1)$$

for some appropriate function $\sigma(X)$. Here the lhs represent a Radon-Nykodyn derivative and $R(X)$ is a boundary term. The [2] relation then follows.

It is easy to see that in the shear flow model $\sigma_\tau = \int_{-\tau}^{\tau} \sigma(X)$ is proportional to the momentum entering the system from the lower wall minus the momentum leaving the system from the upper wall. Due to the conservation of momentum in the bulk of the system the total momentum flux π_τ through the middle of the

system is proportional to σ_τ plus corrections due to the variation of momentum in the upper and lower half of the system. We expect these two quantities to fluctuate much less than the momentum flux, at least if the system is big enough so that we can expect to have a GC fluctuation relation for π_τ ². Similar considerations hold for the heat conduction model.

The deterministic case is far less clear. We know that the average phase-space volume contraction rate is equal to the hydrodynamic entropy production rate, only in some limiting situation, see [12]. Our numerical results, together with those in [21] show that this equality does not extend to their fluctuations. We observe, first of all, that although the CG fluctuation relation appears not to hold $\xi_\tau(p)$ is linear in p so that we can rewrite eq.(2.4) as:

$$\xi_\tau(p) = C_\tau p \quad (5.2)$$

The most striking effect appear to be the divergence of the slope C_τ . A possible explanation of this can be based on the assumption that the distribution $\Pi_\tau(p)$ to be close to a Gaussian, see [BCL], so that

$$C_\tau = \frac{2}{S(\tau)}$$

where

$$S(\tau) = \frac{2}{\tau} \sum_{t=-\tau}^{\tau} D(t) - \frac{2}{\tau^2} \sum_{t=-\tau}^{\tau} |t|D(t) \quad (5.3)$$

is the integral of the π -autocorrelation function $D(t) = \langle \pi(\Phi^t(\cdot))\pi(\cdot) \rangle - \langle \pi \rangle^2$.

Now when $\sum_{t=-\tau}^{\tau} D(t)$ converges to a finite value the GC relation reduces to the usual Green-Kubo relation. On the other hand if we assume that $\sum_{t=-\tau}^{\tau} D(t)$ approaches 0 when $\tau \rightarrow \infty$ then C_τ has to diverge as τ^{-1} , which is in good agreement with our numerical data. We were not able to check more directly this relation due to the lengthy simulations involved but we hope to come back to this in future work.

We already noted that the quantity that enters the GC theorem for our deterministic shear flow model, *i.e.* the phase space contraction rate due to collisions, appears to have little in common with the hydrodynamic entropy production. This is different from models of deterministically boundary thermostated heat conduction systems in which the phase space contraction rate assume the form of an entropy production [1] [4], [13]. We expect that it is possible to introduce a deterministic forcing term for the shear flow acting only at, or near, the boundary and producing a phase space contraction rate equal to the hydrodynamic entropy production, see [12]. This would make the GC relation dependent on the form of the boundary forcing term.

5.2. Local fluctuation

As we already noted in [21] the local fluctuation, in both the stochastic and deterministic case, do not satisfy a fluctuation law in the form of eq.(2.6) but they appear to be in good agreement with the more general relation eq.(2.7). This seems to be contrary to the results obtained in [24] and in [5].

To resolve this apparent contradiction we note that in [24] Gallavotti considers a chain of weakly interacting Anosov dynamical systems³ and takes as a subsystem a finite piece of the chain. The phase space contraction rate is an extensive quantity as in the bulk thermostated systems. Furthermore the correlations in the chain decay exponentially both in space and in time. In a system with these characteristics one can prove that the fluctuation of the phase space contraction rate due to the degree of freedom of the subsystem satisfy a fluctuation relation with corrections proportional to the boundary of the subsystem times the correlation length.

In our situation none of the above characteristics is present. First of all we are not able to divide the degrees of freedom between the subsystem and the rest of the system. Moreover the phase space volume contraction is present only at the boundary of the system and the subsystem does not include any portion of the boundary. Finally we expect the correlation length in our system to be very long (potentially infinite), *i.e.* bigger than the size of the subsystem considered. For these reason we do not expect the arguments in [24] and [5] to be

² We observe however that differently from the analysis in [4] we do not have an a priori bound on the fluctuation of the total momentum of the system.

³ The paper by Maes deals with a rather more general situation but similar arguments apply also there.

applicable to our situation. We observe however that our system is closer to the experimental situation described in [20] and to possible other experiments one can imagine doing.

As in [21] we do not have any real explanation for the apparent validity of eq.(2.7). We think that the GC fluctuation relation can be extended to a partial relation of the form eq.(2.7) in a wide range of situations. These include a system of particles under the influence of an electric field and a Gaussian thermostat, see [22] and [25] for more details. We think that for the asymmetric simple exclusion process, one should be able to find an analytic justification of this behavior.

Acknowledgements We are indebted to E.G.D. Cohen and G. Gallavotti for many helpful discussion and suggestion. Research supported in part by NSF Grant DMR-9813268, and Air Force Grant F49620-98-1-0207.

References.

- [1] G. Gallavotti, “New Methods in Nonequilibrium Gases and Fluids”, Open System and Information Dynamics, Vol. **6**, 101-136 (1999)
- [2] G. Gallavotti, E.G.D. Cohen, “Dynamical ensemble in a stationary states” Jour. Stat. Phys **80**, 931–970 (1995).
- [3] J. Kurchan, “Fluctuation theorem for stochastic dynamics”, Jour. Phys. A **31**, 3719-3729 (1998).
- [4] J.L. Lebowitz, H. Spohn, “A Gallavotti-Cohen-type symmetry in the large deviation functional for stochastic dynamics”, J. Stat. Phys. **95**, 333-365 (1999).
- [5] C. Maes, “The fluctuation theorem as a Gibbs property”, J. Stat. Phys. **95**, 367–392 (1999).
- [6] D.J. Evans, E.G.D. Cohen, G.P. Morriss, “Probability of Second Law Violations in Shearing Steady Flows”, Phys. Rev. Letters **71**, 2401–2404 (1993).
- [7] D. Ruelle, “Dynamical Systems Approach to Nonequilibrium Statistical Mechanics: An Introduction”, IHES/Rutgers, Lecture Notes, 1997.
- [8] D. Ruelle, “Positivity of entropy production in nonequilibrium statistical mechanics” J. Stat. Phys. **85**, 1–23 (1996).
- [9] G. Gentile, “Large deviation rule for Anosov flows”, Forum Math. **10**, 89–118 (1998).
- [10] Moran Hoover, “Diffusion in a periodic Lorentz gas”, J. Stat. Phys. **48**, 709–726 (1987).
- [11] D.J. Evans, E.G.D. Cohen, G.P. Morriss, “Viscosity of a simple fluid from its maximal Lyapunov exponent”, Phys. Rev. A **42** 5990-5997 (1990)
- [12] N.I. Chernov, J.L. Lebowitz, “Stationary Nonequilibrium States for Boundary Driven Hamiltonian Systems” JSP **86**, 953–990 (1997).
- [13] private communication.
- [14] R. Esposito, J.L. Lebowitz, R. Marra, “Hydrodynamic limit of the stationary Boltzmann equation in a slab” Comm. Math. Phys. **160**, 49-80 (1994).
- [15] F. Bonetto, J.L. Lebowitz, L. Rey-Bellet, “Fourier’s Law: a Challenge for Theorists”, Mathematical Physics 2000, Edited by A. Fokas, A. Grigoryan, T. Kibble and B. Zegarlinsky, Imperial College Press, 128-151 (2000).
- [16] S. Goldstein, J.L. Lebowitz and E. Presutti, “Mechanical System with Stochastic Boundaries” Colloquia Mathematica Societati János Bolay **27** 403–419 (1979).

- [17] S. Goldstein, C. Kipnis and N. Ianiro, “Stationary States for a System with Stochastic Boundary Conditions” *J. Stat. Phys.* **41**, 915–930 (1985).
- [18] F. Bonetto, A.J. Kupiainen, J.L. Lebowitz, “Perturbation theory for coupled Arnold cat maps: absolute continuity of marginal distribution”, preprint.
- [19] G. Gallavotti, “Extension of the Onsager’s reciprocity to large fields and the chaotic hypothesis”, *PRL* **77**, 4434-4437 (1996).
- [20] S. Ciliberto, S. Laroche, “An experimental verification of the Gallavotti-Cohen fluctuation theorem”, *Journal de Physique IV* **8**, 215-219 (1998).
- [21] F. Bonetto, N.I. Chernov, J.L. Lebowitz, “(Global and Local) Fluctuation of Phase Space Contraction in Deterministic Stationary Non-Equilibrium, *Chaos* **8**, 823–833 (1998).
- [22] F. Bonetto, G. Gallavotti, P.L. Garrido, “Chaotic principle: an experimental test”, *Physica D* **105**, 226–252 (1997).
- [23] S. Goldstein, J.L. Lebowitz, K. Ravishankar, “Approach to equilibrium in models of a system in contact with a heat bath”, *J. Stat. Phys.* **43**, 303–315 (1986).
- [24] G. Gallavotti, “A local fluctuation theorem”, *Physica A* **263**, 39-50 (1999).
- [25] F. Bonetto, D. Daems, J.L. Lebowit, V. Ricci, “Properties of Stationary Nonequilibrium States in the Thermostated Periodic Lorentz Gas III: The many colliding particles system”, in preparation.